International Journal of Advances in Engineering and Management (IJAEM)
Volume 7, Issue 08 Aug. 2025, pp: 147-156 www.ijaem.net ISSN: 2395-5252

Crossplot Analysis for Viscosity Sensitive Elastic Attributes in Freeman Field, Niger Delta

Ufot, Promise Nkereuwemand Dagogo Tamunonengiyeofori
Center for Petroleum Geoscience, University of Port Harcourt

Date of Submission: 25-07-2025 Date of Acceptance: 05-08-2025

ABSTRACT
Elastic properties were estimated using log data from wells in the Freeman field of Niger Delta. The goal was to investigate the existence of relationships between elastic attributes and reservoir fluid viscosity. The attributes considered include Acoustic impedance, Lambda-rho, VpVs ratio, Poisson ratio and Young modulus and they were estimated using rock physics models. Cross-plots colour coded with the measured viscosity for three different reservoirs were analyzedto determine sensitivity of these elastic attributes to variations in reservoir fluid viscosity.The cross-plot of Lambda-rho versus Poisson ratio revealed that the reservoir with comparatively high viscosity clustered on lower Lambda-rho and higher poisson ratio while the reservoir with the lowest viscosity clustered around higher Lambda-rho and lower Poisson ratio. The cross-plots also revealed that the relatively high vicosity reservoir had higher velocity ratio but lower acoustic impedance and Young modulus while the reservoirs with lower viscosities plotted on higher acoustic impedance and Young modulus but lower Velocity ratio. The analyses showed that some elastic attributes have a level of sensitivity to fluid viscosity, a situation that may be exploited ininferring reservoir fluid viscosities directly from seismic data.
Keywords: Elastic properties. Cross-plots. Viscosity

I. INTRODUCTION

Due to the world's population growth, urbanization, and economic development, the world's energy demands are increasing quickly. The International Energy Agency (IEA) projects that by 2040, the world's energy consumption will have increased by 30%. The oil and gas sector is under a lot of pressure to increase energy production while reducing costs and environmental effects due to this rising demand. More complicated geological environments, such deepwater reservoirs, tight formations (like shale), heavy oil, or tar sand deposits, are often the site of recent oil and gas discoveries. For the oil and gas to be extracted successfully and efficiently in these complicated environments, certain technologies, methods, and knowledge are needed. A significant amount of the oil is usually left in situ by conventional oil recovery techniques including primary and secondary recovery. Recovery efficiency from these techniques may be as low as 10–30%. Enhanced Oil Recovery (EOR) techniques may be necessary to remove the residual oil since it may be challenging.

Viscosity is the fluid parameter that has the most impact on oil production and recovery (Batzle et al., 2006). The energy required to lower the oil's viscosity and enable its flow (such as by cyclic steam stimulation or steam-assisted gravity drainage) increases with the oil's viscosity. Because it influences the flow of oil through the reservoir and production systems, viscosity is a critical component in oil recovery and needs to be taken into account right from the onset, so that suitable planning and financial allocations may be developed to increase the effectiveness of rehabilitation.

Viscosity affects fluid flow, production rates, and improved oil recovery techniques' effectiveness. In order to mobilize and generate the hydrocarbons, high-viscosity fluids, such as heavy oil, often need increased recovery procedures, such as chemical injections or heat treatments. Accurately determining and measuring fluid viscosity is essential in the early phases of exploration and production planning since these enhanced oil recovery methods are sometimes costly and technically complex. Conversely, low-viscosity fluids, such as natural gas and light oil, are much simpler to extract but need accurate characterization to optimize recovery and reduce production costs. Motivated by the need to incorporate all the information possible, in the

International Journal of Advances in Engineering and Management (IJAEM)
Volume 7, Issue 08 Aug. 2025, pp: 147-156 www.ijaem.net ISSN: 2395-5252

process of field development planning, this endeavor has attempted to highlight the possibility of inferring reservoir fluid viscosities from seismic data, by analyzing the sensitivity of elastic attributes estimated from log data to viscosity changes, in the cross-plot domain.

II. GEOLOGY OF THE STUDY AREA

In 1997, the "Freeman field" was identified. It is known for its substantial oil deposits in the Agbada Formation, this offshore field is situated about 120 kilometers (75 miles) southwest of the Niger Delta coastline (Fig. 1 and 2).

This field was chosen because it has a wealth of subsurface data and a well-documented production history, which give the information required to assess the correlation between fluid viscosity and seismic characteristics. With depths ranging from around 900 meters (2950 feet) to 1300 meters (4260 feet), the Freeman Field is known for its deep water location. Since 2005, the Freeman Field's Agbada formation reservoirs have produced around 225,000 barrels of light, sweet oil per day. The entire stack volume, which is around 154 km2 (59.5 square miles), is the 3-D seismic volume that was utilized to describe the research region. With a bin spacing of 6.25 m (21 ft) by 12.5 m (41 ft), the seismic survey has a high resolution. For every stack, the 3-D seismic volume consists of 1160 in-lines (N-S) and 851 crosslines (E-W). Because the wavelet's dominant frequency is 35 Hz, the sedimentary column's average interval velocity of 2300 m/s (7544 ft/s) enables imaging (resolution) of stratigraphic intervals as thin as 16 m (53 ft), even though they are beyond the zone of interest and reach depths of roughly 6000 m (19,680 ft). There were checkshots for five of the wells, logs (GR, Resistivity, Density, Neutron, DT), and seismic reflection data from seven wells (Freeman-001, 002ST3, 003, 003ST1, 004, 004ST1, and 005). According to investigations conducted around the Freeman Field, reservoir deposits are thought to represent turbidites of either base-of-slope fans or intermediate mid-slope fans (Adekanbi, personal communication, 2014). The three main basin formations that make up the stratigraphy of Freeman Field in the Niger Delta are the Benin Formation (continental sands) as the cap rock, the Agbada Formation (paralic sands and shales) as the reservior unit, and the Akata Formation (deep marine shales at the base), which is the main source rock. Notable characteristics of the field include possible overpressure from the underlying Akata Shale, which is often seen in the crestal zone of the field's anticlinal structure, and deformation of the strata brought on by extensional faulting. Collapse crested, back-to-back, and huge, steeply dipping regional flank structural structures are its defining characteristics. On the continental slope, there are many signs of marine shale movement, such as domes, ridges, and diapirs (Doust and Omatsola, 1990).

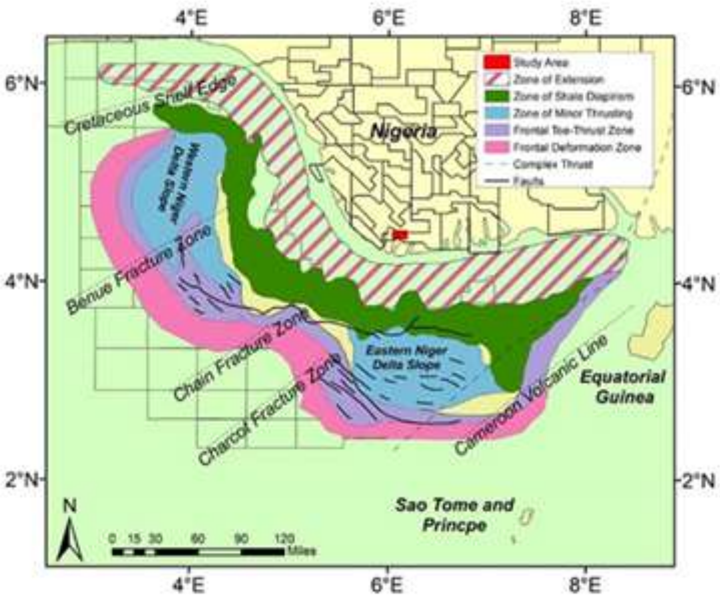

Figure 1: Regional geology of the Deepwater Niger Delta. Adapted from Mabon Limited (2020)

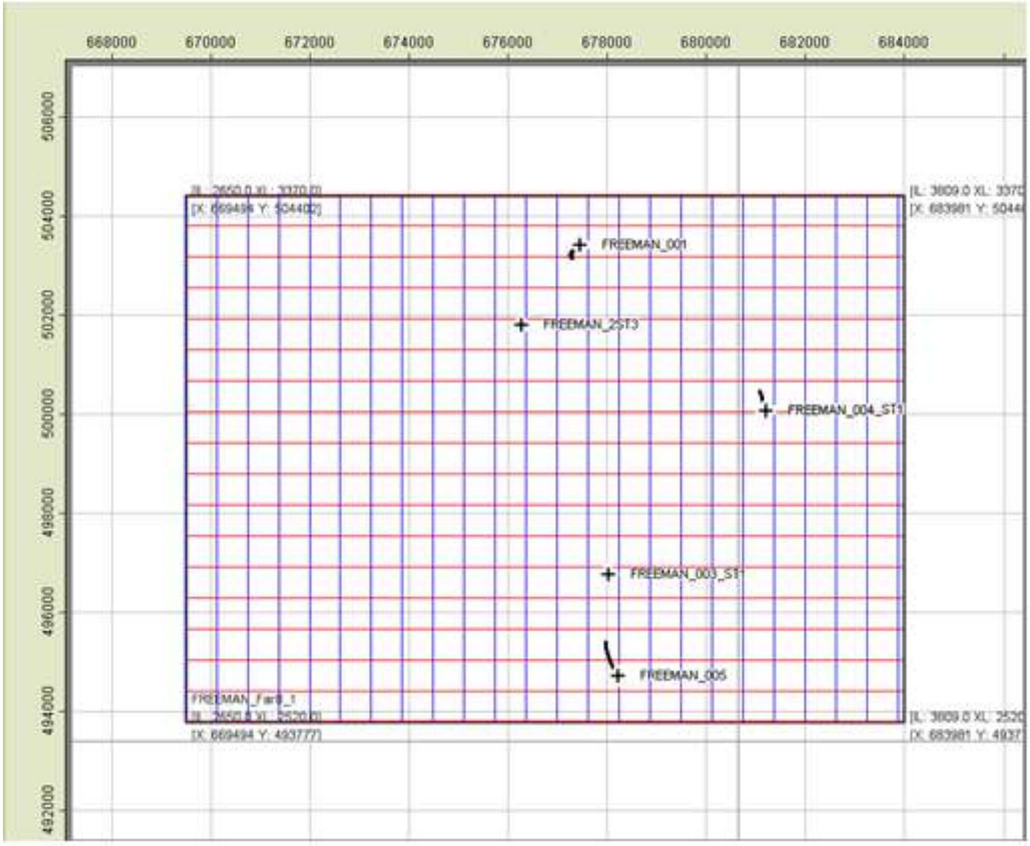

Figure 2: Base Map of the Study area

III. MATERIALS AND METHOD

The materials used in this study include well logs, and PVT data . A combination of different well logs like gamma ray, resistivity, neutron and density logs were used for reservoir delineation. Vp was derived from sonic logs and Vs was predicted from Vp logs. After which acoustic impedance and other elastic properties were calculated using preexisting relationships in literatures (Equation 1-5). Crossplot analysis was then used to display the relationship between these attributes and viscosity. Figure 3 displays the workflow that was used for this studyLambda-rho which is an indicator of the rocks incompressibility. It is a function of acoustic impedance and shear impedance. Lambda-rho was evaluated using Eq.1

$$\lambda\rho = Z^2 - 2SI^2 = \rho(Vp^2 - 2Vs^2) \quad \text{……………………} \quad \text{Eq. 1}$$

Acoustic impedance (Z) which is a measure of how much a material resists sound wave was evaluated using Eq.2

$$Z = \rho * Vp \quad \text{………………………………………………} \quad \text{Eq. 2}$$

Poisson ratio (PR) which is the ratio of the lateral strain to axial strain and is a measure of the amount of lateral deformation of the reservoir under stress. This attribute was evaluated using Eq. 3

$$PR = (Vp^2 - 2Vs^2) / 2(Vp^2 - Vs^2) \quad \text{…………………………} \quad \text{Eq.3}$$

Velocity ratio (VR) which is the ratio of p-wave velocity to s-wave velocity was evaluated using Eq.4

$$VR = Vp/Vs \quad \text{……………………………………………} \quad \text{Eq. 4}$$

Young modulus (E) which is the ratio of the logitudinal stress to longitudinal strain, simply put, it is the measure of a materials stiffness or rigidity. It was evaluated using eq.5

$$E = \rho * Vp^2 * (1- 2*PR) / (1-PR) \quad \text{……………..………} \quad \text{Eq. 5}$$

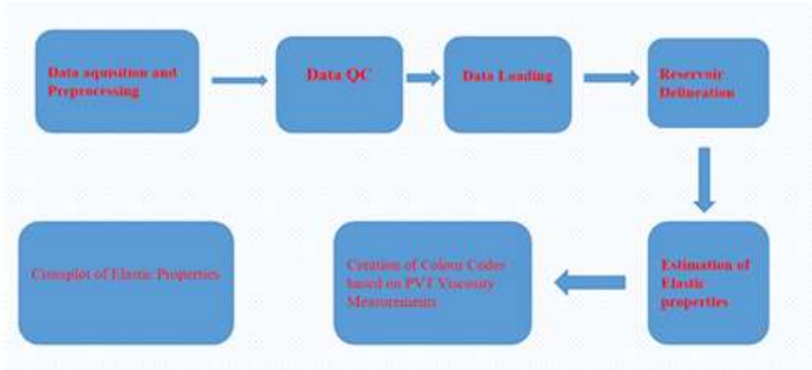

Figure 3 Work flow for this study

IV. RESULTS PRESENTATION

4.1 Reservoir Delineation

Through a combination of gamma ray, resistivity, neutron and density logs, several reservoirs were delineated (Fig. 4) but for the sake of this study, we'll be focusing on three major reservoirs for which PVT data are available. The Freeman field has two major lithologies which are sandstone and shale and the reservoirs are within the sandstone formations. The three reservoirs of interest are reservoir 670 (F-70), 690 (F-90) and 803 (H-03) and are designated as top and base at their respective depths (Table 1).

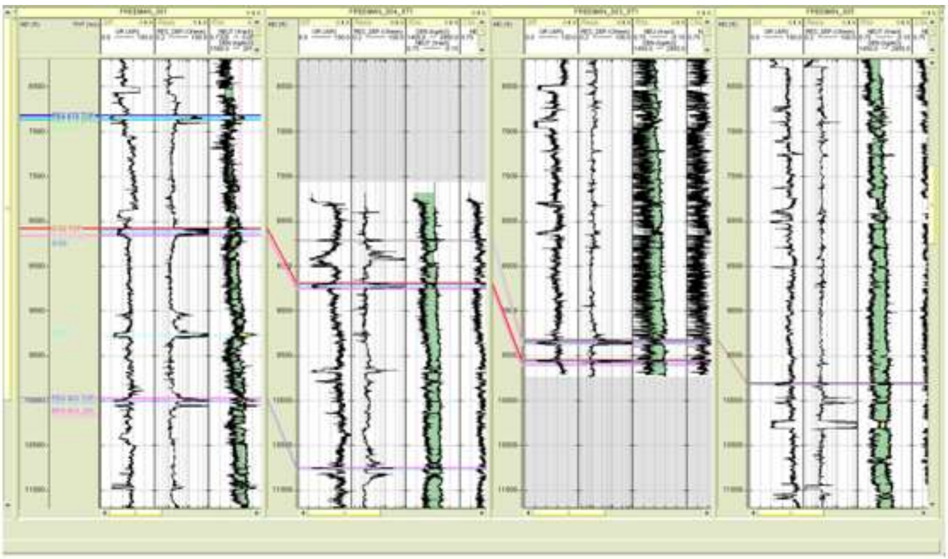

Figure 4: Delineate reservoirs

Table 1 Reservoir top and base

RESERVOIR	TOP (ft)	BASE (ft)	RESERVOIR THICKNESS (ft)	VISCOSITY (cP)
RES 670 (Green)	6816.782	6865.402	48.62	5.062
RES 690 (Yellow)	9319.611	9368.882	49.271	0.931
RES 803 (Pink)	10747.116	10772.02	24.904	0.434

International Journal of Advances in Engineering and Management (IJAEM)
Volume 7, Issue 08 Aug. 2025, pp: 147-156 www.ijaem.net ISSN: 2395-5252

4.2 Crossplot Analysis

Some elasticproperties of the reservoirs, such as acoustic impedance, lambda-rho, velocity ratio, Poisson's ratio and young modulus were estimated and their sensitivity to viscosity evaluated in cross plot space.The cross plots were color coded with the known viscosity values of the different reservoirs, as shown inTable 1. The green color represents RES 670 with a viscosity of 5.062 cP, the yellow represents RES 690 with viscosity of 0.931 cP while the pink represents RES 803 with a viscosity of 0.434 cP.

Figure 5 and 6 are cross plots of Lambda-rho against Poisson ratio, for Res 670 (green) and Res 803 (pink) and Res 670 (green) and Res 690 (yellow), respectively.The relatively high viscosity reservoir (green) plots on lower Lambda-rho values (>0.010 to <0.015GPa_kg/m3) and higher Poisson ratio values (0.4 to 0.45), while the relatively lower viscosity reservoir (pink) plots on higher lambda-rho values (<0.015 to >0.02GPa_kg/m3) and lower Poisson's ratio values (0.3 to <0.4).

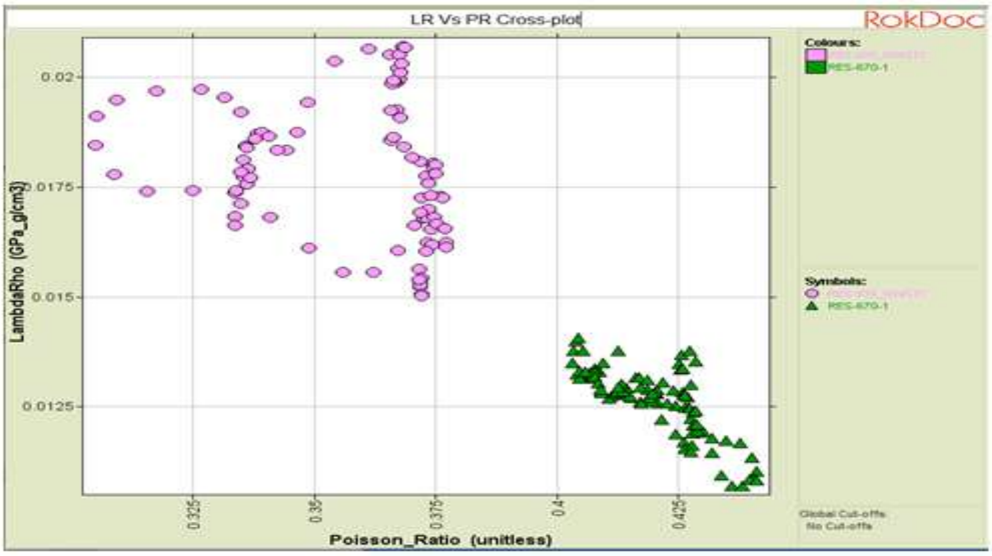

Figure 5 Lambda-rho and Poisson ratio crossplot

In Figure 6, the relatively high viscosity reservoir (green) plots on lower Lambda-rho values (<0.01 to 0.015GPa_kg/m3) and higher poison ratio values (0.4 to 0.45), while the medium viscosity reservoir (yellow) plots on higher lambda-rho values (>0.0125 to 0.0175GPakg/m3) and lower Poisson's ratio values (0.35 to <0.4).

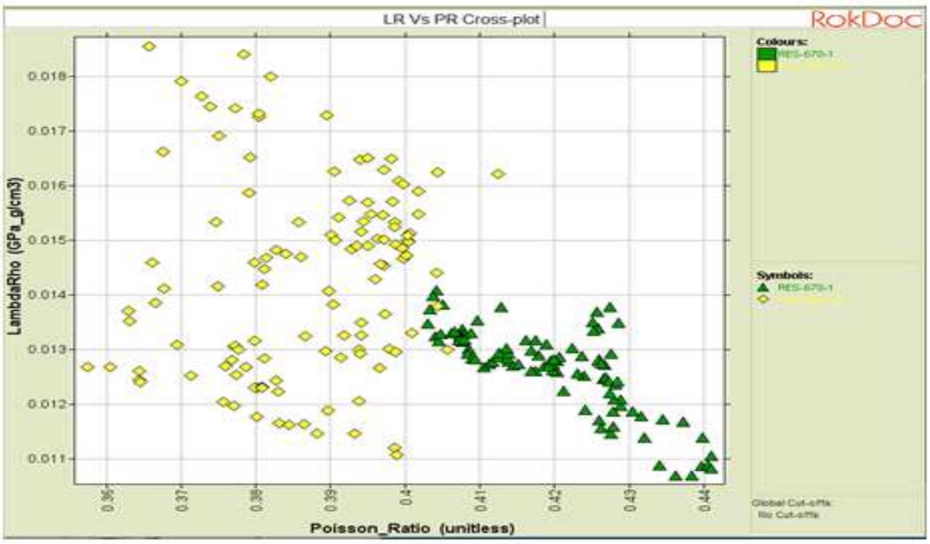

Figure 6: Lambda-rho and Poisson ratio crossplot

Figure 7 is a crossplot of acoustic impedance againstpoisson ratio,for the highest and lowest viscosities. As established earlier for poisson ratio, the green reservoir plots on high poisson ratio values (0.4 to 0.45) and lower acoustic impedance values (>2.5e6 to 5e6 kg/m3_m/s) while the pink reservoir plots on lower poisson ratio (0.3 to <0.4) and higher acoustic impedance values (>5e6 to 7.5e6 kg/m3_m/s). A crossplot of these same attributes using the three reservoirs (Fig. 8) displays the degree of separation between these reservoirs as viscosity increases.

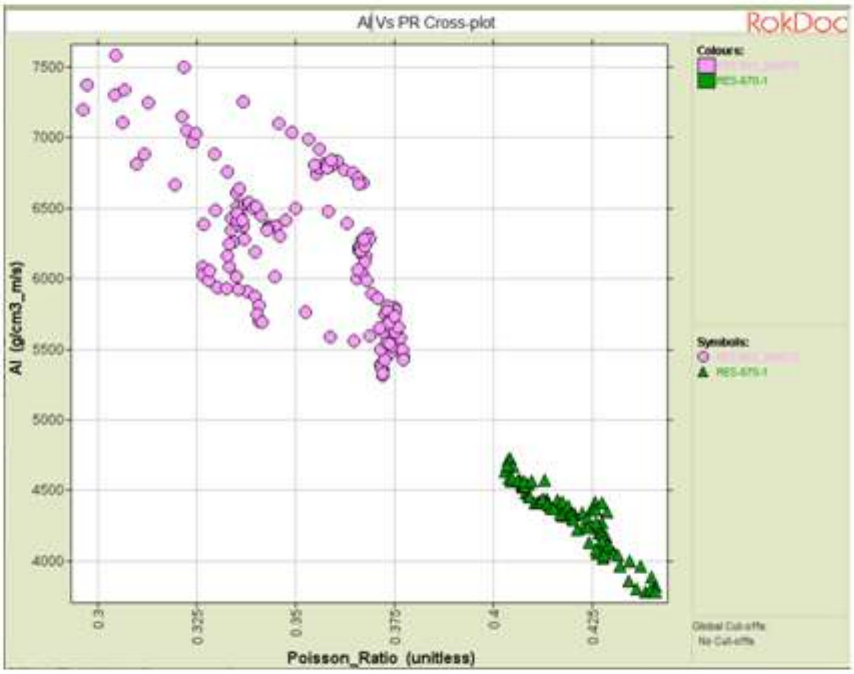

Figure 7: Acoustic impedance and Poisson ratio crossplot

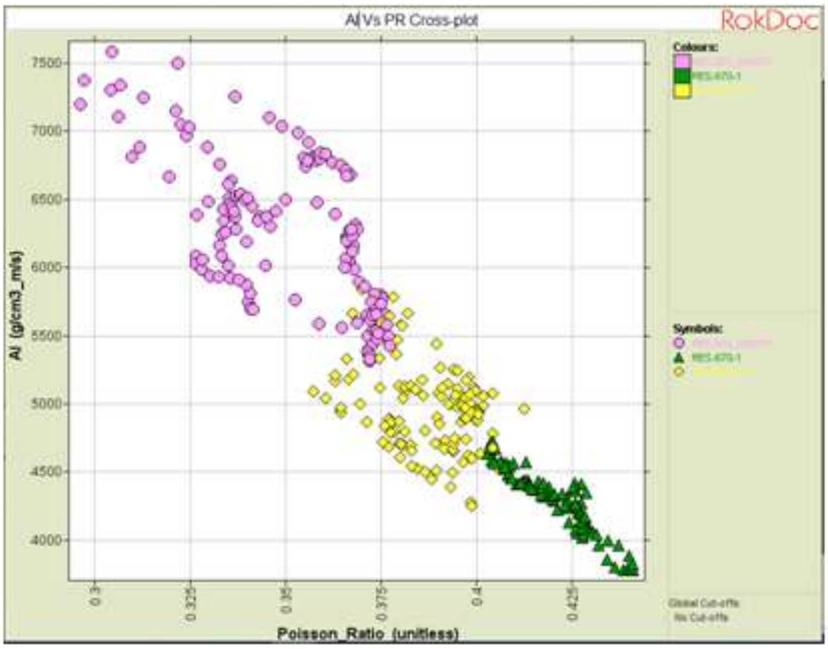

Figure 8: Acoustic impedance and Poisson ratio crossplot

International Journal of Advances in Engineering and Management (IJAEM)
Volume 7, Issue 08 Aug. 2025, pp: 147-156 www.ijaem.net ISSN: 2395-5252

A crossplot of acoustic impedance and lambda-rho was done using the green and pink reservoirs (Fig. 9). these reservoirs cluster on same values as earlier established for both acoustic impedance and lambda-rho. Highest viscosity (Green) plots on lower lambda-rho and lower acoustic impedance while lowest viscosity (pink) plots on higher lamda-rho and higher acoustic impedance values.

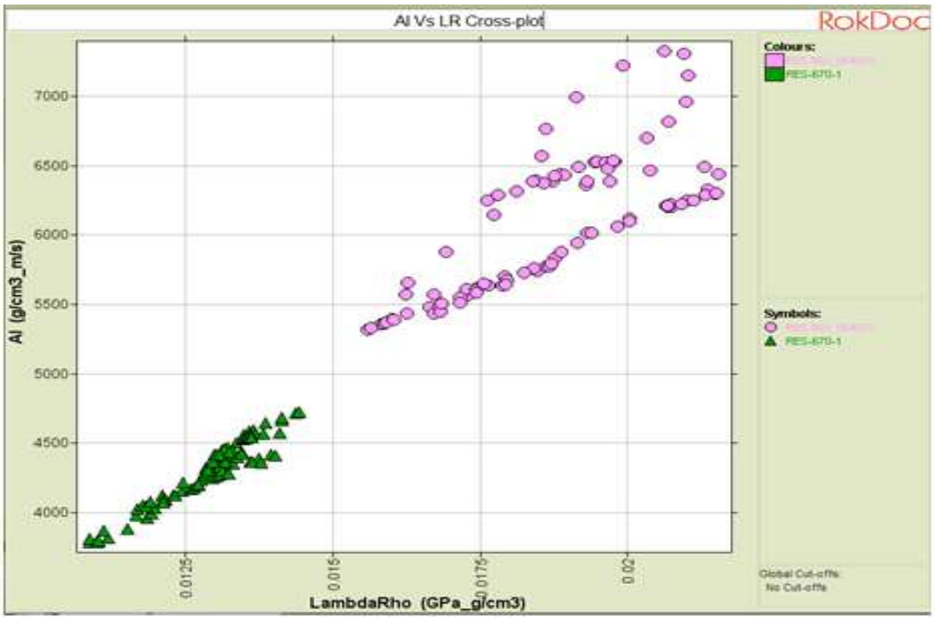

Figure 9: Acoustic impedance and Lambda-rho crossplot

Figure 10 is a crossplot of Young modulus (E) and Poisson ratio. The relatively high viscosity reservoir (green) and the relatively low viscosity reservoir (yellow) were clearly separated by both the Poisson ratio and Young modulus (E).Lower E values (<5e6 GPa) and higher poisson ratio values (0.4 to 0.45) plots correspond to the relatively high viscosity reservoir (green), while the comparatively lower viscosity reservoir (yellow) plots higher E values (>1.5e7 GPa) and lower poisson values (>0.35 to 0.4).

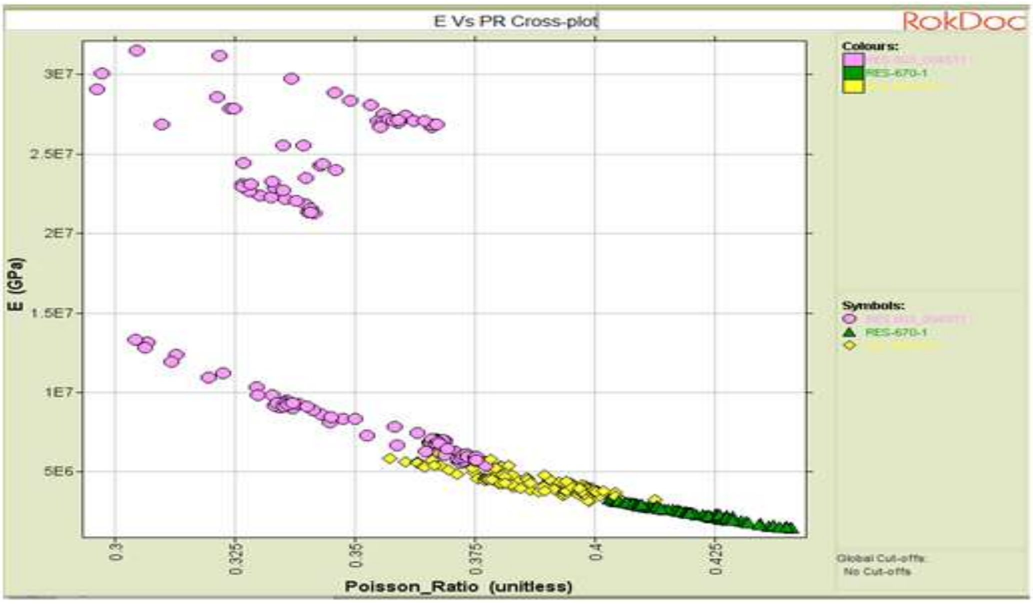

Figure 10: Young modulus and Poisson ratio crossplot

International Journal of Advances in Engineering and Management (IJAEM)
Volume 7, Issue 08 Aug. 2025, pp: 147-156 www.ijaem.net ISSN: 2395-5252

Two reservoirs (RES 670 (green) and RES 803(pink)) with known viscosity values of 5.062cP and 0.434cP, respectively, were used to create a cross plot of Lambda-rho and velocity ratio (Fig.11). The relatively high viscosity reservoir (green) and the relatively low viscosity reservoir (pink) were clearly separated by both Lambda-rho and velocity ratio, indicating that both are viscosity-sensitive. The comparatively low viscosity reservoir (pink) plots on lower velocity ratio values (⩽ 2.25) and greater lambda-rho values (>7e10 GPa_kg/m3) while the relatively high viscosity reservoir (green) plots on higher velocity ratio (Vp/Vs) values (>2.5) and lower lambda-rho values (⩽ 1.5e10 GPa_kg/m3).

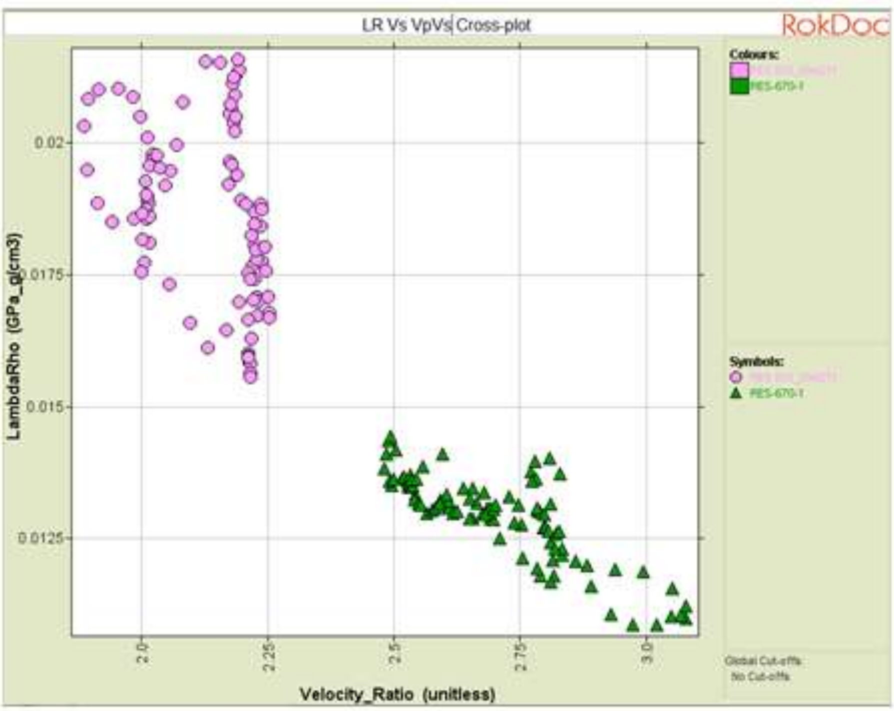

Figure 11: Lambda-rho and Velocity ratio crossplot

V. DISCUSSION OF RESULTS

The results show that the elastic properties whose sensitivity to viscosity were assessed, showed appreciable sensitivity to viscosity, as reservoirs with relatively different viscosities were well discriminated in the cross plot space. The lambdarho, Poisson’s ratio, VpVsand acoustic impedance, showed better sensitivity compared to the young’s modulus. The most notable separations based on viscosity differences, however, are shown by the LambdaRho, velocity ratio, and poisson ratio.Fluids with relatively high viscosity are observed to have lower LambdaRho values, while fluids with relatively low viscosity are linked to higher LambdaRho values. Considering the theoretical expression for lambda-rho, given as $\lambda\rho = AI^2 - CSI^2$,this may be thought of as a consequence of a possible introduction ofa little resistance to shearingin the high viscosity fluid, which, in conjunction with the shear impedance of the rock, lowers the Lamdba-rho value,whensubtracted from the composite rock attribute, acoustic impedance.The comparatively high viscosity hydrocarbon reservoir had lower values for the young modulus (E),a measurement of a rock's resistance to deformation under stress, whereas the relatively low viscosity hydrocarbon had higher values. Since high viscosity fluids tend to have higher compressibilities than low viscosity fluids, their presence reservoir rocks tend to reduce the rock’s resistance todilatation and makes it more prone to deformation, the poisson's ratio which is a measure of the rock's propensity to deform in a brittle or ductile manner, tends to be lower for the relatively low viscosity fluid and higher for the relatively high viscosity fluid. Because the velocity ratio and poisson's ratio are closely related, their crossplot findings are comparable. The findings are consistent with the theory that certain seismic characteristics may be used to forecast viscosity; the most useful indicators were found to be Vp/Vs, Poisson ratio, and Lambdarho. Though other factors may have some influence on the observed results, such as depth, geomechanicaldisposition and provenance and diagenetic history, their effect can be discounted by the degree of discrimination observed in cross plot space.

VI. CONCLUSION OF FINDINGS

In a bid to establish the possibility of predicting the viscosity of hydrocarbons, using seismically derivable elastic properties, certain elastic attributes were estimated from well logs and analysed in cross plot space. Conclusively, the findings show good sensitivity of some elastics parameters to variations in the viscosity of reservoir fluids. Fluids with low and comparatively high viscosities were clearly distinguished by Lambda-rho, Vp/Vs, AI, Young modulus and Poisson's Ratio. This gives the promise that field wide viscosity variation can be mapped effectively from seismic data, by employing inversion schemes to generate volumes of these viscosity sensitive elastic parameters.

Acknowledgements I want to sincerely acknowledge and appreciate my supervisor Dr. T. Dagogo for his contributions and encouragement towards the success of this study. A big thank you to Mr. A. Enwemadu and my family for their unwavering support.

Data Availability The datasets used for this study are not publicly available due the confidentiality agreement signed with the oil company operating in the study area that provided the datesets for this study but are available from the corresponding author on reasonable request.

Declaration

Competing interests The authors declare no competing interests.

REFERENCES

[1]. Adewoye, O. O., Aizebeokhai, A. P., and Olayinka, A. I. (2015). Reservoir characterization using well log and 3D seismic data: Offshore Niger Delta as a case study. Ifẹ Journal of Science, 17(3), 789–802.

[2]. Asef, M. R., and Najibi, A. (2013). Rock physics investigation of seismic wave absorption in reservoir rocks. Global Journal of Geological Sciences, 11(1), 1–10. https://doi.org/10.4314/gjgs.v11i1.1

[3]. Avseth, P., Mukerji, T., and Mavko, G. (2005). Quantitative seismic interpretation: Applying rock physics tools to reduce interpretation risk. Cambridge University Press.

[4]. Avseth, P., Mukerji, T., and Mavko, G. (2010). Quantitative seismic interpretation: Applying rock physics tools to reduce interpretation risk. Cambridge University Press.

[5]. Connolly, P. J. (1999). Elastic impedance. Geophysics, 64(3), 809–818. https://doi.org/10.1190/1.1444607

[6]. De Ghetto, G., Villa, M., and Dal Piaz, D. (1995). Experimental PVT and viscosity modeling for heavy and extra-heavy oils. Society of Petroleum Engineers International Heavy Oil Symposium. https://doi.org/10.2118/30285-MS

[7]. Doyen, P. M. (2007). The impact of rock properties on seismic attributes and their correlation with reservoir viscosity. Geophysics, 72(5), E127–E135. https://doi.org/10.1190/1.2747731

[8]. Dvorkin, J., and Nur, A. (1996). Rock physics model correlating bulk modulus and viscosity: Implications for seismic interpretation. Geophysics, 61(5), 1079–1087. https://doi.org/10.1190/1.1444047

[9]. Ekine, A. S., and Ibe, A. O. (2013). Delineation of reservoir structure using well log and seismic data in parts of the Niger Delta. Journal of Geosciences and Geomatics, 1(1), 1–6. https://doi.org/10.12691/jgg-1-1-1

[10]. Ellis, D. V., and Singer, J. M. (2008). Well logging for earth scientists (2nd ed.). Springer.

[11]. Elphick, J. (1987). Well logging for earth scientists. Elsevier Applied Science.

[12]. Khalid, A., Ahmed, M., Shuaib, M., and Al-Marzouqi, A. (2015). Integration of rock physics and seismic inversion for facies prediction in a tight reservoir. SEG Technical Program Expanded Abstracts 2015, 2874–2878. https://doi.org/10.1190/segam2015-5928794.1

[13]. Lawrence, R. D., Nelson, J. R., and Ambrose, G. W. (2002). Lithostratigraphy and depositional environment of the Niger Delta. In G. R. L. Clark (Ed.), Niger Delta Petroleum System (pp. 9–25). AAPG Memoir.

[14]. Mann, G., Maynard, J., and Oliver, W. (2002). The effect of temperature on the viscosity of hydrocarbon fluids and its impact on mobility. Journal of Petroleum Science and Engineering, 33(3), 231–241. https://doi.org/10.1016/S0920-4105(02)00033-2

[15]. Mavko, G., Mukerji, T., and Dvorkin, J. (2009). The rock physics handbook: Tools for seismic analysis of porous media (2nd ed.). Cambridge University Press.
[16]. McKennell, W. G. (1956). The nature and measurement of viscosity. Reinhold Publishing Corporation.
[17]. Mehrotra, A. K., and Svrcek, W. Y. (1986). The effect of temperature and pressure on the viscosity of hydrocarbon fluids. Journal of Canadian Petroleum Technology, 25(5), 54–61. https://doi.org/10.2118/86-05-04
[18]. Najibi, A., and Asef, M. R. (2014). Rock-physics-based estimation of critical-clay-volume fraction and its effect on seismic velocity and petrophysical properties. Geophysics, 79(3), D175–D185. https://doi.org/10.1190/geo2012-0510.1
[19]. Ohakwere-Eze, O., Olayinka, A., and Ibe, C. (2018). Application of density and gamma-ray crossplots, along with Vp/Vs ratios, to delineate lithologies in the Niger Delta. Journal of African Earth Sciences, 146, 77–89. https://doi.org/10.1016/j.jafrearsci.2018.07.002
[20]. Okoli, D., Chikwendu, C., and Olorunfemi, A. (2018). Application of rock property crossplots to detect gas in the Soku Field. Journal of Natural Gas Science and Engineering, 59, 103–113. https://doi.org/10.1016/j.jngse.2018.08.003
[21]. Okeugo, V., Adeoti, L., and Ojo, T. (2017). Validation of elastic attribute crossplots in predicting rock quality and reservoir continuity. Journal of Geophysics and Engineering, 14(6), 1462–1474. https://doi.org/10.1088/1742-2140/aa8f7b
[22]. Pickett, G. R. (1963). Acoustic impedance and the characterization of reservoir rocks. Geophysics, 28(6), 929–938. https://doi.org/10.1190/1.1439246
[23]. Reijers, T. J. A., Petters, S. W., and Nwajide, C. S. (1997). The Niger Delta Basin. In R. C. Selley (Ed.), African basins (Vol. 3, pp. 151–172). Elsevier
[24]. Rider, M., and Kennedy, M. (2011). The geological interpretation of well logs (3rd ed.). Whittles Publishing.
[25]. Short, K. C., and Stauble, A. J. (1967). Outline of the geology of the Niger Delta. AAPG Bulletin, 51(5), 761–779.
[26]. Stacher, K. (1995). The Niger Delta petroleum system: Stratigraphy, sedimentology, and depositional environments. In: The Petroleum Geology of the Niger Delta, 51(6), 761–779.
[27]. Tuttle, M. L. W., Charpentier, R. R., and Brownfield, M. E. (1999). The Niger Delta Petroleum System: Niger Delta Province, Nigeria, Cameroon, and Equatorial Guinea, Africa. U.S. Geological Survey Open-File Report 99-50-H. https://pubs.usgs.gov/of/1999/ofr-99-0050/HOFR-99-50-H/
[28]. Weber, K. J., and Daukoru, E. M. (1975). Petroleum geology of the Niger Delta. In N. Wright and T. L. Dickey (Eds.), Proceedings of the Ninth World Petroleum Congress (Vol. 2, pp. 209–221). Applied Science Publishers.
[29]. Weber, K. J. (1986). The petroleum geology of the Niger Delta Basin. In R. C. Selley (Ed.), African Basins (Vol. 3, pp. 135–156). Elsevier.
[30]. Zhang, H., Castagna, J. P., and Chen, X. (2013). Seismic estimation of hydrocarbon viscosity using rock physics principles. Geophysics, 78(6), D403–D408. https://doi.org/10.1190/geo2013-0022.1